Thermochimica Acta, 236 (1994) 249–262
Elsevier Science Publishers B.V., Amsterdam
SSDI 0040-6031(93)01596-U

Non-isothermal kinetic and thermodynamic study of the decomposition of lead acetate trihydrate

M.A. Mohamed *, S.A. Halawy and M.M. Ebrahim
Department of Chemistry, Faculty of Science, Qena, Egypt

(Received 28 November 1992; accepted 8 September 1993)

Abstract

The non-isothermal decomposition of lead acetate trihydrate was studied up to 450°C by means of TG, DTG, DTA and DSC measurements in a dynamic atmosphere of N_2 (or dry air).

The parent salt was found to undergo melting concurrently with the dehydration process, which takes place in two steps between 30 and 110°C. The anhydrous salt melts at 204°C and later forms two intermediate basic lead acetate salts, namely $Pb(CH_3COO)_2 \cdot PbO$ (between 230 and 270°C) and $Pb(CH_3COO)_2 \cdot 2PbO$ (between 275 and 325°C) respectively. The latter basic salt decomposes, between 325 and 380°C in N_2 atmosphere, to produce a mixture of PbO and a small amount of metallic Pb. In air, however, the decomposition produces solid PbO only.

X-ray powder diffraction and IR transmission spectroscopy were used to identify the solid intermediates and products of the reaction. Gas chromatography was used to identify the volatile products of the decomposition in N_2 and in O_2. Scanning electron microscopy was also used to investigate the structure changes and possible occurrence of melting during the decomposition.

Values of the kinetic (ΔE and ln A) and thermodynamic (ΔH, C_p and ΔS) parameters were calculated for the dehydration and decomposition processes.

INTRODUCTION

The thermal decomposition of metal acetates, under various conditions, has been the subject of numerous studies [1, 2]. This is partly due to the fact that acetates, in particular those of the transition metals, represent a common precursor for the preparation of a wide range of metals and metal oxide catalysts, some of which are of industrial importance [3]. In addition, metal acetates are common surface intermediates, and a knowledge of their thermal behaviour is important for understanding processes involving adsorption [4] and surface reactions [5]. In the decomposition of metal malonates [6, 7] and acetyl acetonates [8], the corresponding metal acetates are also formed as reaction intermediates.

* Corresponding author.

Several studies have been published on the decomposition of lead acetate trihydrate [9–14]. A detailed description of its decomposition is reported to be incomplete [9]. Decomposition in N_2 atmosphere was reported [12] to produce acetone, CO_2, acetic acid, H_2O and H_2. In addition, acetic anhydride, acetylacetone and ketene have also been reported [14] as decomposition products. The residual solid is composed of metallic Pb and a small percentage of PbO in N_2 atmosphere, while in air, PbO is the only solid product [13]. Two basic acetate salts are formed as reaction intermediates, $Pb(CH_3COO)_2 \cdot PbO$ at 240°C and $Pb(CH_3COO)_2 \cdot 2PbO$ at 305°C [14].

Liebold and Huber [14] have found that the dehydration process of lead acetate trihydrate was not clear on the TG curve but appeared on the DTA curve as a broad endotherm with two maxima. They used elemental analysis and X-ray diffraction to characterize the two reaction intermediates. The anhydrous lead acetate was reported [14] to melt at 206°C with no appreciable weight loss.

The present investigation is intended to extend our work on some transition metal acetates and to study, in detail, the complete decomposition course of lead acetate trihydrate.

EXPERIMENTAL

Material and techniques

The lead acetate trihydrate, $Pb(CH_3COO)_2 \cdot 3H_2O$, used in the present study was analytical grade material (Riedel-DeHaen AG Seelze, Hanover, Germany).

Thermal analyses, i.e. thermogravimetry (TG), differential thermal analysis (DTA) and differential scanning calorimetry (DSC) were performed using Shimadzu (Japan) instruments (TGA-50H, DTA-50 and DSC-50). These instruments were supplied with a data processor which gives values of the temperatures, weight loss and the amount of heat involved in each thermal event. In addition, it also supplies the DTG curve for each TG experiment.

Experiments were carried out in a dynamic atmosphere of dry N_2 (40 ml min^{-1}). Dry air was also used in some experiments. Highly sintered α-Al_2O_3 powder (Shimadzu Co.) was used as a reference material for the DTA and DSC measurements. The heat of transition (28.24 J g^{-1} [15]) of pure indium metal (Johnson Matthey) at 157°C was adopted for the DSC calibrations.

Constant weights of sample (namely 10–15 mg) were used in order to avoid the effect of variation in sample weight on the peak shape and temperature.

X-ray powder diffraction analysis of lead acetate and the solid products of its calcination at various temperatures was carried out by means of a

model JSX-60PA Jeol diffractometer (Japan) equipped with a source of Ni-filtered Cu Kα radiation. Results were matched with ASTM standard cards.

Gas-phase decomposition products of anhydrous lead acetate were analysed using a Shimadzu computerized gas chromatograph, model GC-14A, connected with a flow system at atmospheric pressure. Dry N_2 (or dry O_2) was used as a dynamic atmosphere (85 ml min^{-1}) and as a carrier. Analysis was carried out with SUS, column PEG 6000 10% on shimalite TPA, 60/80 mesh, 3 mm I.D. × 2 m at 150°C. Product gases were sensed by a thermal conductivity detector (TCD). Automatic sampling was performed with a heated gas sample cock, type HGS-2.

IR transmission spectroscopy of the solid decomposition products at some selected temperatures were performed by means of a Perkin-Elmer 1430 ratio-recording IR spectrometer.

Data analysis

Kinetic parameters, i.e. the activation energy (ΔE in kJ mol^{-1}) and the frequency factor (ln A), were calculated for the dehydration and also for the decomposition steps, using the Kissinger equation [16]

$$\frac{d(\ln \phi/T_m^2)}{d(1/T)} = \frac{-E}{R}$$

where ϕ is the heating rate (°C min^{-1}), T_m the DTA peak temperature and R the gas constant (8.314 J mol^{-1} $°C^{-1}$).

Accordingly, linear plots of $\ln \phi/T_m^2$ versus $1/T$ were constructed, and then the slope and intercept values were used to derive ΔE and $\ln A$: slope $= -E/R$ and the intercept $= \ln AR/E$.

Thermodynamic parameters, ΔH, C_p and ΔS, for each process were calculated from the DSC curves. The enthalpy change ΔH values were given directly from the amount of heat involved in each process (in kJ mol^{-1}). The heat capacity C_p for each process was obtained from the equation [17]

$$C_p = \Delta H/\Delta T$$

where $\Delta T = T_2 - T_1$, and T_1 is the temperature at which the DSC peak begins to leave the baseline, whereas T_2 is the temperature at which the DSC peak returns.

The entropy change ΔS is calculated using the equation [17]

$$\Delta S = 2.303 C_p \log T_2/T_1$$

RESULTS AND DISCUSSION

Thermal analyses

Thermogravimetry (TG) and differential thermal analysis (DTA) were carried out for the decomposition of lead acetate trihydrate at five different

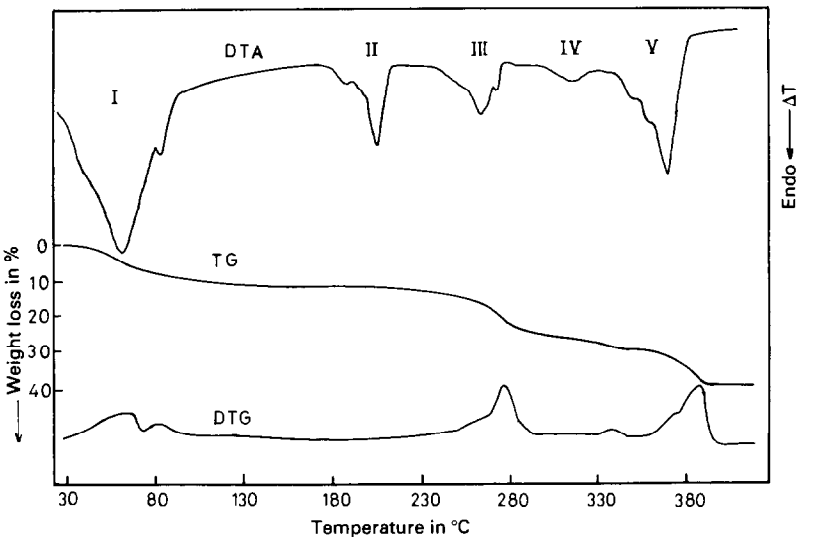

Fig. 1. TG, DTG and DTA curves for the thermal decomposition of $Pb(CH_3COO)_2 \cdot 3H_2O$, performed at a heating rate of 10°C min^{-1} in a dynamic atmosphere of N_2 (40 ml min^{-1}).

heating rates, approx. 5, 7, 10, 15 and 20°C min^{-1}, in a dynamic atmosphere of dry N_2 (40 ml min^{-1}).

Figure 1 shows TG, DTG and DTA curves recorded at 10°C min^{-1} up to 450°C. The TG curve displays four weight loss steps. The first step is located between 30 and 110°C and is accompanied by a weight loss of 11.64% of the original weight of the sample. This step accounts for the dehydration process of the trihydrated salt, although the weight loss measured here (approx. 11.64%) is slightly less, by 2.6%, than expected ($3\,H_2O$ are equivalent to 14.25% of the molecular weight of the salt). We attribute this discrepancy to the evolution of some water of hydration at ambient temperature, see the TG curve; the loss in weight started immediately at the beginning of measurements. This behaviour resembles that of $NiCl_2 \cdot 6H_2O$ [18]. There is a gradual slight decrease in weight, after the dehydration process, up to 184.5°C. The second step takes place between 184.5 and 285°C with 13.4% weight loss. The third step follows in the temperature range 285–342.5°C and is accompanied by a weight loss of 5.8%. Finally, the fourth step appears between 342.5 and 390°C with 11.05% weight loss. This makes a total weight loss of 41.9% of the original weight of sample after completion of the decomposition process. This suggests that the final solid product is composed of PbO and a small percentage of metallic Pb (PbO alone would require a 41.1% weight loss, while metallic Pb alone would require a weight loss of 45.4%).

The DTG curve, Fig. 1, shows five peaks which are maximized at 64.9, 80.9, 277.6, 336.6 and 387.7°C. The first two peaks correspond to the

TABLE 1

Summary of the TG and DTG results

Heating rate ϕ/ °C min^{-1}	1st process			2nd process		3rd process		4th process		Total
	T_{max}/°C		Wt. loss %	T_{max}/°C	Wt. loss %	T_{max}/°C	Wt. loss %	T_{max}/°C	Wt. loss %	Wt. loss %
	1	2								
5	58.8	70.0	11.96	206.1	13.8	318.2	4.75	370.5	10.70	41.21
7	64.5	74.9	11.87	268.9	13.6	335.9	5.31	379.2	11.31	42.09
10	64.9	80.9	11.64	277.6	13.4	336.6	5.78	387.7	11.05	41.86
15	65.6	86.2	11.78	279.0	13.4	341.4	5.81	392.8	10.86	41.82
20	66.4	86.5	12.72	291.4	13.5	348.1	6.02	399.7	10.67	42.94

dehydration process (first step in TG curve). Table 1 summarizes the TG and DTG results at different heating rates.

The DTA curve, Fig. 1, shows five main endothermic processes (**I–V**), some of which are split into two peaks, and which are maximized at 55.1, 204.7, 263.3, 318 and 368.2°C. The first, broad, endotherm, **I**, at 55.1°C has a small, sharp shoulder at 81.1°C. This process corresponds to the first step in the TG curve (with 11.64% weight loss) and, therefore, is attributed to the dehydration process (which is known [14] to take place in two consecutive steps, see also the two DTG peaks at 64.9 and 80.9°C) and to a possible melting of the partially dehydrated salt. The sharp endotherm, **II**, at 204.7°C, is not accompanied by any appreciable weight loss, Fig. 1. It is ascribed [14] to melting of the anhydrous lead acetate [$Pb(CH_3COO)_2$].

The third endotherm, **III**, at 263.3°C, corresponds to the second TG step, with 13.4% weight loss, and is attributed [14] to the decomposition of the anhydrous lead acetate to form the intermediate basic acetate salt, $Pb(CH_3COO)_2 \cdot PbO$. The measured weight loss for this step (approx. 13.4%) is not far from the theoretical calculations (15.69%).

The endothermic peak **IV**, at 318°C, is broad and weak. It corresponds to the third step in the TG curve, which was accompanied by 5.8% weight loss. This peak can be attributed [14] to the decomposition of the intermediate salt $Pb(CH_3COO)_2 \cdot PbO$ to form another basic acetate salt, $Pb(CH_3COO)_2 \cdot 2PbO$. This is in good agreement with the theoretical calculations which should result in 6.2% weight loss. Finally, the endothermic process **V** is composed of two peaks at 363.7 and 368.2°C and is attributed to the decomposition of the intermediate $Pb(CH_3COO)_2 \cdot 2PbO$ to produce the residual solid mixture of PbO + Pb.

Table 2 indicates the shifts towards higher temperatures in DTA peak-maximum temperatures T_{max} as a result of variation in the rate of heating ϕ of the lead acetate.

The effect of the prevailing atmosphere on the decomposition process was studied. Two identical DTA experiments (at 10°C min^{-1}, using the same

TABLE 2

Summary of the DTA results

Heating rate ϕ/ °C min^{-1}	Dehydration		Decomposition			
	Endo I		Endo II	Endo III	Endo IV	Endo V
	1	2				
5	48.6	64.2	202.3	250.3	—	356.7
7	53.8	80.3	204.0	252.9	310.0	363.7
10	55.1	81.1	204.7	263.3	318.0	368.2
15	63.1	81.5	206.1	267.2	328.4	375.3
20	64.9	82.0	207.0	273.7	334.6	383.6

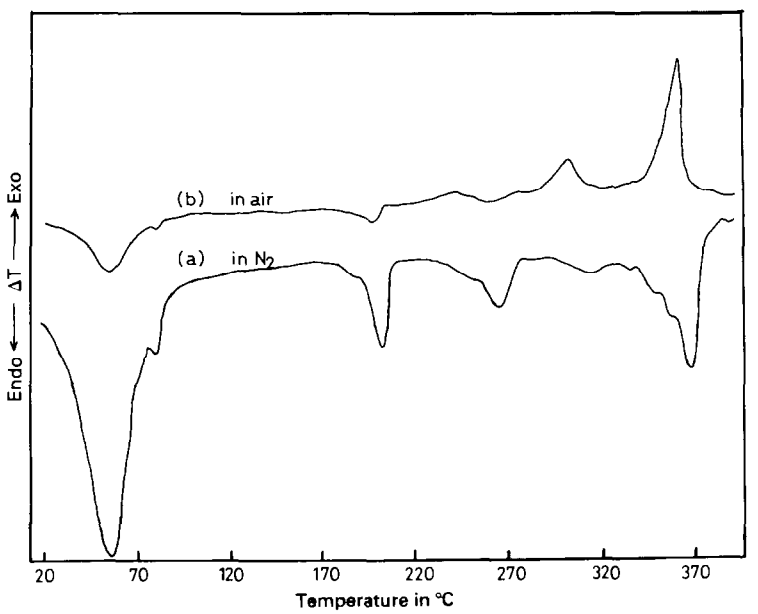

Fig. 2. DTA curves for the decomposition of $Pb(CH_3COO)_2 \cdot 3H_2O$, performed at a heating rate of 10°C min^{-1}: curve (a) in N_2; curve (b) in air (40 ml min^{-1}).

weight of sample) were performed. Dry N_2 atmosphere was used in one experiment while dry air was used in the second (the same rate of flow, 40 ml min^{-1}, was used). Figure 2 shows the results obtained. The first three processes (**I–III**) have not changed, i.e. they are endothermic in both atmospheres. The last two processes, **IV** and **V**, however, became exothermic in air atmosphere, having been endothermic in N_2. This could be explained as an enhanced oxidation which, in turn, will increase the amount of PbO present in the final residual solid.

TABLE 3

Summary of the kinetic and thermodynamic parameters for the decomposition of lead acetate trihydrate

Parameter	Dehydration I		Decomposition			
	Step 1	Step 2	II	III	IV	V
ΔE/kJ mol^{-1}	67.83	432.10	542.10	123.67	115.20	172.42
ln(A min^{-1})	24.44	148.55	107.51	27.21	22.51	31.64
Corr. coeff.	0.999	0.989	0.833	0.982	0.999	0.993
ΔH/kJ mol^{-1}	95.07		11.68	26.21	6.35	36.67
C_p/kJ °C^{-1} mol^{-1}	01.30		0.32	0.42	0.15	0.60
ΔS/kJ °C^{-1} mol^{-1}	1.77		0.058	0.103	0.021	0.103

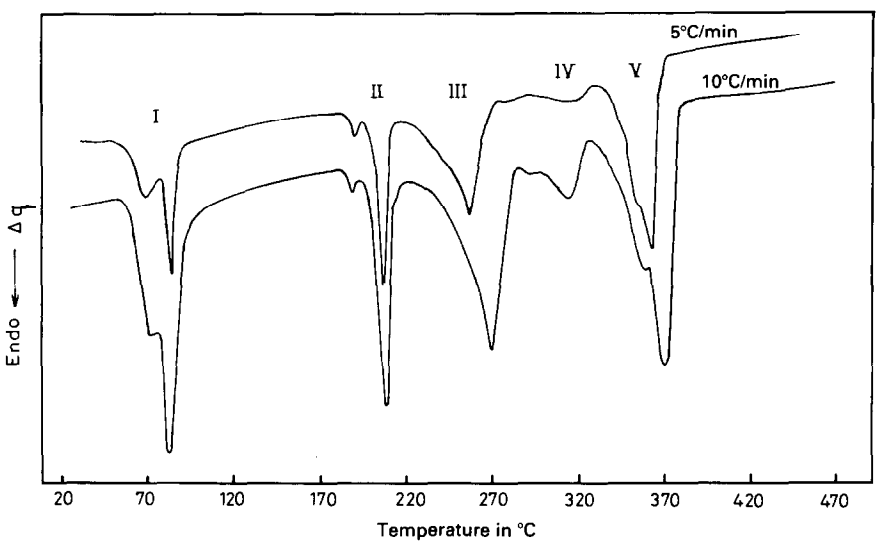

Fig. 3. DSC curves for the decomposition of $Pb(CH_3COO)_2 \cdot 3H_2O$ at heating rates of 5 and 10°C min^{-1} in an atmosphere of N_2 (40 ml min^{-1}).

The data in Table 2 were used to calculate the activation energy ΔE and the frequency factor ln A using the method described above. These values together with the correlation coefficient for each line are listed in Table 3.

Figure 3 shows two DSC curves that were recorded in N_2 at 5 and 10°C min^{-1}. There is a clear similarity in shape between the DSC and DTA curves. Each DSC curve is composed of five main endothermic peaks, some of which are split with two overlapping maxima. These DSC curves, and others, were used to calculate thermodynamic parameters, i.e. the enthalpy change ΔH, heat capacity C_p and the entropy change ΔS, for the dehydration and the decomposition steps. These values are listed in Table 3.

Scanning electron microscopy (SEM)

Scanning electron microscopy was used to investigate the parent lead acetate as well as the samples that were heated in N_2 at some selected temperatures within the range of our study. Figure 4 (a)–(c) shows three representative micrographs that were taken at different stages of the reaction.

Micrograph (a) shows crystallites of the parent salt, (magnification $\times 150$), which are characterized by an irregular shape, a relatively rough surface and the appearance of some cracks. These features are indicative of an early evolution of some water of crystallization prior to study. This was apparent earlier in the discrepancy in the weight loss accompanying the dehydration process (see TG results).

Micrograph (b) shows a sample which has been heated at 140°C in N_2 ($\times 350$). It shows clearly that the salt has suffered extensive melting, displaying rounded edges and pores. These rounded structures are thought [19] to be controlled by surface tension. The cracks located at the bottom left of the micrograph may have resulted from strain developed during cooling of the salt after reaction.

Micrograph (c) shows a sample that was heated in N_2 at 330°C ($\times 750$). It shows some elongated, rather thin, crystallites of different sizes of the intermediate basic salt, $[Pb(CH_3COO)_2 \cdot 2PbO]$, which was shown by X-ray diffraction to be formed between 385 and 342°C, see also the TG results.

Melting measurements

The results of the SEM investigation, which showed melting features for the sample heated at 140°C, suggested a careful analysis of the behaviour of the reactant on heating by means of a melting point apparatus. Two melting processes were observed for the lead acetate salt. The first started at 58°C and the salt remained in the molten state, with evolution of gases up to 130°C, where a solid was formed. This was followed by the second melting step at 204°C; the reaction continued in the melt up to >270°C where a solid product began to precipitate.

These observations agree with the features seen in the SEM micrographs and, in addition, explain the high values of activation energy ΔE calculated for the process overlapping with the dehydration and, also, for endotherm II (at 204.7°C), see Table 3.

Product analysis

Solid phase products

X-ray diffraction. Figure 5 exhibits four X-ray powder diffractograms obtained for the solid calcination products of lead acetate heated in N_2 at

(a)

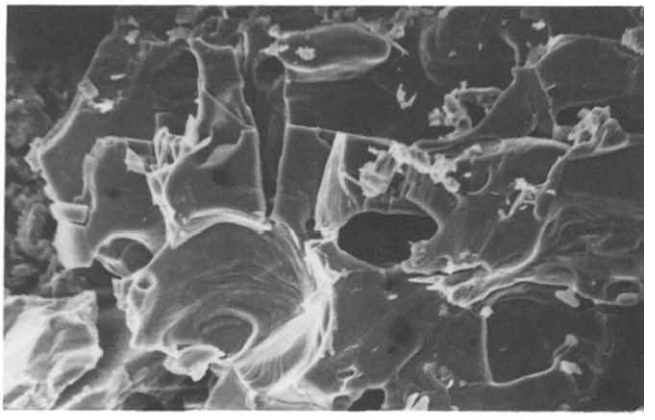

(b)

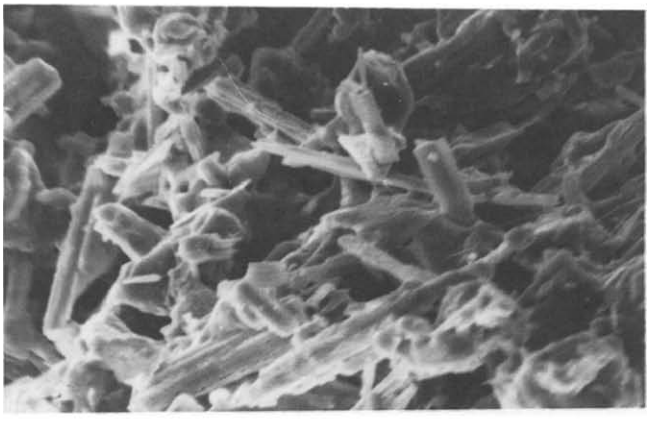

(c)

Fig. 4. Scanning electron micrographs for samples of lead acetate at different stages of decomposition: a, the parent material (original magnification × 150); b, sample heated at 140°C (original magnification × 350); c, sample heated at 330°C (original magnification × 750).

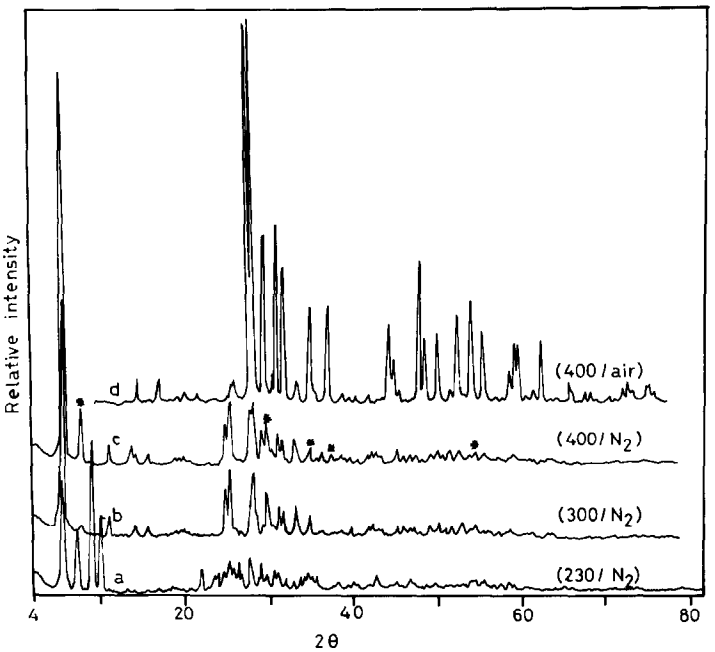

Fig. 5. XRD powder diffractograms for the solid phase decomposition products of lead acetate trihydrate at the temperatures indicated for 60 min: samples a–c were heated in N_2; sample d was heated in air.

230 (a), 300 (b) and 400°C (c) together with a sample heated in air at 400°C (d).

The pattern shown in diffractogram (a) indicates the formation of the basic salt, i.e. $Pb(CH_3COO)_2 \cdot PbO$, with its *d*-spacing values at 12.45, 8.4, 7.62, 3.80 3.35 and 2.92 Å [14]. Diffractogram (b), however, suggests the formation of another basic acetate which has the formula $Pb(CH_3COO)_2 \cdot 2PbO$. The pattern of this matches well with the reported [14] *d*-spacing values at 7.14, 5.72, 5.22, 4.19, 3.40, 3.34, 3.06, 2.88, 2.76, 2.71, 2.60, 2.25 and 2.08 Å.

Diffractogram (c) shows a pattern that matches well the standard red PbO (ASTM card 5-0561) with the appearance of some lines (labelled *) characteristic of Pb metal (ASTM card 4-0686). The last diffractogram (d) shows the pattern of PbO alone.

The X-ray diffraction results are in line with the TG results which suggested that two basic salts are produced as reaction intermediates. One is formed between 230 and 286°C, i.e. $Pb(CH_3COO)_2 \cdot PbO$, and the other between 286 and 327°C, i.e. $Pb(CH_3COO)_2 \cdot 2PbO$.

IR spectroscopy. Figure 6 shows four IR transmission spectra of the parent lead acetate hydrate (a) and of the solid calcination products on heating the salt at 290°C (b), 340°C (c) and 400°C (d) in N_2 atmosphere.

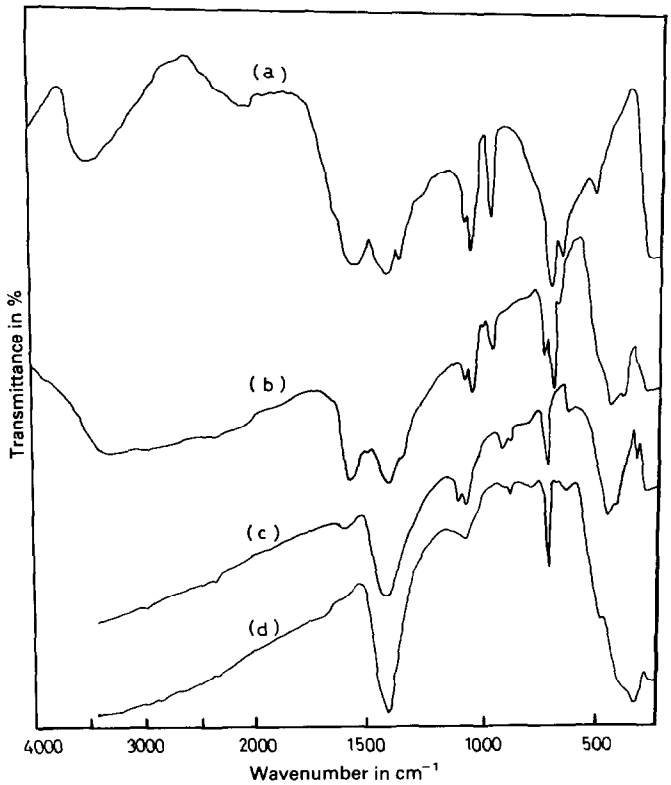

Fig. 6. IR spectra of the parent lead acetate trihydrate (a) and the solid phase products of its heating at: (b) 290°C; (c) 340°C; and (d) 400°C, in N_2 atmosphere for 60 min.

The parent salt (a) shows the characteristic absorptions of the acetate anion [20] at 950, 670, 620 and 500 cm^{-1}. A broad band characteristic of water of hydration is seen between 3600 and 3100 cm^{-1} [21]. In addition, absorption bands attributed [21] to carboxylate anion between 1610 and 1550 cm^{-1}, and 1430 and 1300 cm^{-1} are also shown.

In spectra (b) and (c), the absorption band attributed to water of crystallization had disappeared. The absorption bands attributed to acetate are still present but their intensities are relatively decreased with increasing decomposition temperature. A new absorption band appears in both spectra, between 300 and 500 cm^{-1}; this is assigned to the formation of PbO [22] and agrees well with the X-ray and TG results which suggested that two basic salts were formed at these calcination temperatures; both of these salts contain PbO in their structures. Some other absorption peaks at 1050, 1020, 940, 930, 860, 666 and 620 cm^{-1} are attributed to the formation of basic lead acetate [23].

Spectrum (d), the solid product at 400°C, shows the absorption band of PbO below 500 cm^{-1} and, in addition, some absorption peaks at 1407, 1047,

844 and 685 cm^{-1}. These peaks are attributed to the presence of $PbCO_3$ [20].

To determine whether $PbCO_3$ is a product of the decomposition or if it was formed as a result of the reaction between the product PbO and the atmospheric CO_2 after the decomposition reaction (and before recording the spectrum), two IR spectra were recorded for the solid product after heating to 400°C in N_2. One was recorded immediately and the other was taken after 3 days. The results confirmed that $PbCO_3$ is not a product of the decomposition of the parent salt.

Gas phase products

Gas chromatography was used to identify the volatile decomposition products in an atmosphere of dry N_2 as well as in dry O_2. The main products were identified as acetone, CO_2 and acetic acid. In addition, some other minor products such as CO, ethyl acetate and propionic acid were also detected. Figure 7 shows the distribution of these volatile products in N_2 (a) and in O_2 (b).

In O_2, the relative composition of the volatile products is not affected by the calcination temperature. In N_2, however, the concentration of acetone decreases with temperature while that of acetic acid increases; and CO_2 varies with calcination temperature in an irregular manner.

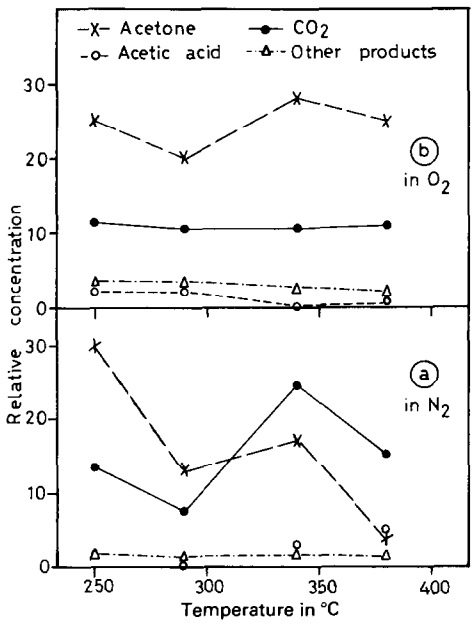

Fig. 7. Distribution of the volatile gaseous products of the thermal decomposition of $Pb(CH_3COO)_2 \cdot 3H_2O$ in: (a) dry N_2; and (b) dry O_2. The flow rate was 85 ml min^{-1}.

It is worth mentioning here that no catalytic reactions took place over the PbO product. This was concluded from a simple experiment in which acetone was passed over freshly prepared PbO (made by heating lead acetate to 400°C): GC detected nothing but acetone.

CONCLUSIONS

The composition of lead acetate trihydrate can be described in five events, as seen from the DTA and DSC curves, which can be summarized as follows.

(i) Event **I** (55–111°C) represents two dehydration steps; the second step involves melting and is accompanied by a high ΔE value, see Table 3.

(ii) Event **II** (185–222°C) is accompanied by no appreciable weight loss. It represents melting of the anhydrous $Pb(CH_3COO)_2$ [14], and is associated, again, with a high ΔE value, see Table 3.

(iii) Event **III** (230–286°C) represents decomposition of the anhydrous salt to produce a basic acetate salt, $Pb(CH_3COO)_2 \cdot PbO$, and volatile products.

(iv) Event **IV** (286–327°C), in which the basic salt formed in Event **III** is decomposed to produce a second basic lead acetate, of composition $Pb(CH_3COO)_2 \cdot 2PbO$, and volatile products.

(v) Event **V** (327–390°C), in which final event, $Pb(CH_3COO)_2 \cdot 2PbO$ decomposes to PbO + Pb and volatile products (which were identified as acetone, CO_2, acetic acid, CO, ethyl acetate, propionic acid, etc.).

The formation of acetone as a primary gaseous product of the decomposition of lead acetate, rather than acetic acid, is a typical behaviour of acetates of irreducible metals [1]. Not all metal acetates produce reactive gas–solid interfaces [1, 2].

The use of the complementary technique of scanning electron microscopy is invaluable because it detects melting processes [19] which may accompany the decomposition reaction of a solid.

REFERENCES

1 A.K. Galwey, S.G. McKee, T.R.B. Mitchell, M.E. Brown and A.F. Bean, Reactivity of Solids, 6 (1988) 173.
2 S.A.A. Mansour, G.A.M. Hussein and M.I. Zaki, Reactivity of Solids, 8 (1990) 197.
3 D.L. Trimm, Design of Industrial Catalysts, Chemical Engineering Monographs 11, Elsevier, Amsterdam, 1980.
4 D.M. Griffiths and C.H. Rochester, J. Chem. Soc. Faraday Trans. 1, 74 (1987) 403.
5 M.I. Zaki and N. Sheppard, J. Catal., 80 (1983) 114.
6 A.K. Galwey and M.A. Mohamed, Solid State Ionics, 42 (1990) 135.
7 A.K. Galwey, S.G. McKee, T.R.B. Mitchell, M.A. Mohamed, M.E. Brown and A.F. Bean, Reactivity of Solids, 6 (1988) 187.
8 H.M. Ismail, J. Anal. Appl. Pyrol., 21 (1991) 315.
9 F. Wohler, Justus Liebigs Ann. Chem., 29 (1839) 63.

10 J. Petersen, Ber. Bunsenges., Z. Elektrochem., 20 (1914) 328.
11 H.G. Denham, J. Chem. Soc., 115 (1919) 109.
12 W. Kronig, Z. Angew. Chem., 37 (1924) 667.
13 K. Manabe and T. Kubo, Kogyo Kagaku Zasshi, 69 (1966) 1733.
14 R. Leibold and F. Huber, J. Therm. Anal., 18 (1980) 493.
15 R.C. Weast (Ed.), Handbook of Chemistry and Physics, 62nd edn., CRC Press, Florida, 1982.
16 H.E. Kissenger, J. Anal. Chem., 29(11) (1957) 1702.
17 C. Heald and A.C.K. Smith, Applied Physical Chemistry, Macmillan Press Ltd., London, 1982, p. 20–40.
18 M.A. Mohamed and S.A. Halawy, J. Therm. Anal., in press.
19 A.K. Galwey, M.A. Mohamed and D.S. Cromie, Reactivity of Solids, 1 (1986) 235.
20 J.R. Ferraro, Low Frequency Vibrations of Inorganic and Coordination Compounds, Plenum Press, New York, 1971.
21 S. F. Dyke, A. J. Floyd, M. Sainsbury and R.S. Theobald, Organic Spectroscopy – An Introduction, 2nd edn., Longman, London, 1978.
22 N.T. McDevitt and W.L. Baun, Spectrochim. Acta, 20 (1964) 799.
23 P. Baraldi, Spectrochim. Acta Part A, 38(1) (1982) 51.